International Journal of Engineering Science 49 (2011) 311–321

Contents lists available at ScienceDirect

International Journal of Engineering Science

journal homepage: www.elsevier.com/locate/ijengsci

On the thermodynamic requirement of elastic stiffness anisotropy in isotropic materials

T. Fuller *, R.M. Brannon

University of Utah, Mechanical Engineering, 50 S. Central Campus Drive, Salt Lake City, UT 84121, United States

ARTICLE INFO

Article history:
Received 8 September 2010
Accepted 31 December 2010
Available online 26 January 2011

Keywords:
Anisotropy
Elasticity
Thermodynamics
Validation
Calibration

ABSTRACT

In general, thermodynamic admissibility requires isotropic materials develop reversible deformation induced anisotropy (RDIA) in their elastic stiffnesses. Taking the elastic potential for an isotropic material to be a function of the strain invariants, isotropy of the elastic stiffness is possible under distortional loading if and only if the bulk modulus is independent of the strain deviator and the shear modulus is constant. Previous investigations of RDIA have been limited to applications in geomechanics where material non-linearity and large deformations are commonly observed. In the current paper, the degree of RDIA in other materials is investigated. It is found that the resultant anisotropy in materials whose strength does not vary appreciably with pressure, such as metals, is negligible, but in materials whose strength does vary with pressure, the degree of RDIA can be significant. Algorithms for incorporating RDIA in a classical elastic–plastic model are provided.

Published by Elsevier Ltd.

1. Introduction

When subjected to large distortions, initially isotropic materials respond by developing anisotropy in their response to deformation. Well-known examples of inelastic deformation-induced anisotropy (IDIA) include directional anisotropy in cold worked metals (Hill, 1948), plastic flow induced anisotropy (Stouffer & Bodner, 1979), and nucleation and growth of oriented micro-cracks in brittle media (Kachanov, 1982; Horii & Nemat-Nasser, 1983). Not to be confused with inherent anisotropy, such as in fiber reinforced composite materials or single crystals, deformation-induced anisotropy is caused by loading and is manifest in changes in the isotropy of the fourth-order tangent stiffness tensor of the material.

In addition to the above mentioned examples of nonrecoverable deformation-induced anisotropy, the first and second laws of thermodynamics imply that the fourth-order tangent stiffness tensor of initially isotropic media develop generally *recoverable* deformation-induced anisotropy (RDIA). This consequence of thermodynamics is known in the applied mechanics community (cf. Marsden & Hughes, 1994; Willam, 2002), and the violation of thermodynamic principles resulting from the adoption of a non-constant shear modulus in an isotropic elastic stiffness was described by Zytynski, Randolph, Nova, and Wroth (1978) who showed that if the shear modulus of elastic materials is allowed to vary with pressure, as commonly assumed in geomaterials, it is possible to construct elastic cycles closed in stress that are not closed in strain. If deformed in a particular manner, a net energy increase is possible – a clear violation of the first law of thermodynamics for elastic adiabatic loading. Zytynski asserted that his analysis lead to one of two alternatives: (1) adopt a constant shear modulus and allow Poisson's ratio to vary with deformation, allowing for Poisson's ratio to become negative, or (2) abandon the notion of an elastic region of material behavior. Zytynski failed to consider a third alternative: allowing the elastic stiffness to develop reversible anisotropy in response to deformation.

* Corresponding author.
E-mail address: timothy.fuller@utah.edu (T. Fuller).

0020-7225/$ - see front matter Published by Elsevier Ltd.
doi:10.1016/j.ijengsci.2010.12.017

Houlsby (1985) describes the theoretical difficulties of modeling pressure-dependence of the shear modulus in clays in a thermodynamically admissible manner. Attention is paid to the fact that coupling of isotropic and deviatoric responses through the pressure-dependence of the shear modulus also requires dependence of the bulk modulus on the stress deviator. In particular, Houlsby notes that pressure-dependence of the shear modulus cannot be simplistically achieved through pressure-dependence of the bulk modulus and constancy of Poisson's ratio. Instead, thermodynamics requires additional terms, in the form of deformation-induced anisotropy. Isotropic–deviatoric coupling in isotropic materials in the context of RDIA has also been described by Hueckel, Tutumluer, and Pellegrini (1992) and Scheidler (1996). More recently, in the theory of hyperplasticity (Borja, Tamagnini, & Amorosi, 1997; Collins & Houlsby, 1997; Einav & Puzrin, 2004; Houlsby, Amorosi, & Rojas, 2005), RDIA plays an implicit role through cross anisotropic terms in the elastic stiffness and compliance.

Outside of the geomechanics community, evidently RDIA has seen little, if any, consideration. In metals plasticity, for example, material nonlinearity is observed (Burakovsky, Greeff, & Preston, 2003; Richmond & Spitzig, 1980) and based on the observation that the ratio of flow strength to shear modulus is approximately constant, pressure dependence of the shear modulus is inferred from experimental data (Guinan & Steinberg, 1975; Hua, Jing, Hua, & Hu, 2002). Pressure-dependence of the shear modulus is also inferred from recordings of ultrasonic shear wave speeds taken at varying pressures. However, material data are still interpreted in the context of elastic stiffness isotropy (Hayes, Hixson, & McQueen, 1999). Evidently, RDIA has never been considered in the context of metals plasticity.

In this paper, the thermodynamic requirement that isotropic materials develop RDIA is emphasized and the degree of RDIA in isotropic materials is quantified. The outline of this paper is as follows: an alternative proof of the thermodynamic requirement of RDIA in the elastic stiffness of isotropic materials is given in Section 2. Algorithms for incorporating RDIA in a classical elastic–plastic framework are given in Section 3, and the degree RDIA in isotropic media is quantified in Section 4.

1.1. Independent and dependent variables

Throughout this paper, strain is regarded as the independent variable. Thus, constraints are developed on the elastic stiffness and moduli on volume change and distortion. By the chain rule, these constraints can be readily cast in terms of stress. Inversion of the elastic stiffness gives similar constraints on the elastic compliance.

2. Elasticity in isotropic media

If a material is capable of elastic behavior, a necessary condition of thermodynamic admissibility is that the stress be derivable from a strain energy potential (Malvern, 1969)

$$\bar{\boldsymbol{\sigma}} = \left(\frac{\partial u(\bar{\boldsymbol{\epsilon}}, \eta, q_k)}{\partial \bar{\boldsymbol{\epsilon}}}\right)_{\eta, q_k}, \tag{1}$$

where u is the internal energy per unit reference volume, $\bar{\boldsymbol{\epsilon}}$ is the strain measure[1] work conjugate to the stress tensor $\bar{\boldsymbol{\sigma}}$, η is the specific entropy, and q_k are internal state variables which change only with dissipation. For an isotropic material, the stress remains invariant under rotation, requiring that

$$\bar{\boldsymbol{\sigma}} = \boldsymbol{w}(\bar{\boldsymbol{\epsilon}}, \eta) = \boldsymbol{w}(\boldsymbol{Q} * \bar{\boldsymbol{\epsilon}}, \eta) = \boldsymbol{Q} * \boldsymbol{w}(\bar{\boldsymbol{\epsilon}}, \eta), \tag{2}$$

where $\boldsymbol{w} = \partial u / \partial \bar{\boldsymbol{\epsilon}}$, and $*$ represents the Rayleigh product, defined for second-order tensors as

$$\boldsymbol{Q} * \boldsymbol{A} = \boldsymbol{Q} \cdot \boldsymbol{A} \cdot \boldsymbol{Q}^{\mathrm{T}}. \tag{3}$$

For a tensor of arbitrary order, the Rayleigh product is defined analogously as

$$(\boldsymbol{Q} * \mathcal{A})_{ij\cdots kl} = \sum_{i=1}^{3} Q_{iq} \cdots Q_{jn} \mathcal{A}_{n\cdots qo\cdots p} Q_{kp} \cdots Q_{lo}. \tag{4}$$

By the representation theorom of isotropic functions (Smith, 1971), the valued tensor function $\boldsymbol{w}$ may be expressed as

$$\boldsymbol{w}(\bar{\boldsymbol{\epsilon}}, \eta) = w_1 \boldsymbol{\delta} + w_2 \bar{\boldsymbol{\gamma}} + w_3 \bar{\boldsymbol{h}}, \tag{5}$$

where $\boldsymbol{\delta}$ is the second-order identity tensor, $\bar{\boldsymbol{\gamma}}$ is the deviatoric part of $\bar{\boldsymbol{\epsilon}}$, $\bar{\boldsymbol{h}}$ is the deviatoric part of $\bar{\boldsymbol{\gamma}} \cdot \bar{\boldsymbol{\gamma}}$, and the ω_i are scalar functions of the "mechanics" invariants of $\bar{\boldsymbol{\epsilon}}$, defined for any second order tensor $\boldsymbol{A}$ as

$$J_1^{\boldsymbol{A}} = \operatorname{tr} \boldsymbol{A}, \quad J_2^{\boldsymbol{A}} = \frac{1}{2} \operatorname{tr} \boldsymbol{A}' \cdot \boldsymbol{A}', \quad J_3^{\boldsymbol{A}} = \frac{1}{3} \operatorname{tr} \boldsymbol{A}' \cdot \boldsymbol{A}' \cdot \boldsymbol{A}', \tag{6}$$

where $\boldsymbol{A}'$ is the deviatoric part of $\boldsymbol{A}$.

[1] The definition of the strain tensor is intentionally left ambiguous so that the following results can be considered general in nature. In specific applications, of course, the strain tensor $\bar{\boldsymbol{\epsilon}}$ would take on a specific meaning and the corresponding stress tensor would necessarily by its work conjugate. For example, if $\bar{\boldsymbol{\epsilon}}$ is the Lagrange strain, then its work conjugate stress would be the 2nd Piola–Kirchhoff stress tensor.

Alternatively, the ω_i can be chosen as functions of any other set of independent invariants of $\bar{\boldsymbol{\epsilon}}$, in which case the tensor basis can also change to any linearly independent triplet that span tensors commuting with $\bar{\boldsymbol{\epsilon}}$. As can be readily verified by back substitution, (5) implies that the internal strain energy of an isotropic material is a function of the mechanics invariants of $\bar{\boldsymbol{\epsilon}}$. Mathematically, $u = u(J_1^{\bar{\epsilon}}, J_2^{\bar{\epsilon}}, J_3^{\bar{\epsilon}}, \eta)$ and the fourth-order elastic stiffness tensor of an isotropic material is found by

$$\mathbb{C} = \left(\frac{\partial^2 u(J_1^{\bar{\epsilon}}, J_2^{\bar{\epsilon}}, J_3^{\bar{\epsilon}}, \eta)}{\partial} \bar{\boldsymbol{\epsilon}} \partial \bar{\boldsymbol{\epsilon}} \right)_{\eta}. \tag{7}$$

Performing the indicated differentiation, the most general form of the elastic stiffness tensor of an isotropic material is

$$\mathbb{C} = \frac{\partial^2 u}{\partial \bar{\boldsymbol{\epsilon}} \partial \bar{\boldsymbol{\epsilon}}} = 3u_{11}\mathbb{E}^{\mathrm{iso}} + u_2\sqrt{5}\mathbb{E}^{\mathrm{sd}} + u_{12}(\bar{\boldsymbol{\gamma}}\boldsymbol{\delta} + \boldsymbol{\delta}\bar{\boldsymbol{\gamma}}) + u_{22}\bar{\boldsymbol{\gamma}}\bar{\boldsymbol{\gamma}} + u_{13}(\bar{\boldsymbol{h}}\boldsymbol{\delta} + \boldsymbol{\delta}\bar{\boldsymbol{h}}) + u_{23}(\bar{\boldsymbol{h}}\bar{\boldsymbol{\gamma}} + \bar{\boldsymbol{\gamma}}\bar{\boldsymbol{h}}) + u_{33}\bar{\boldsymbol{h}}\bar{\boldsymbol{h}} + u_3\mathcal{L}(\bar{\boldsymbol{h}}\boldsymbol{\delta} + \boldsymbol{\delta}\bar{\boldsymbol{h}}), \tag{8}$$

where u_i and u_{ij} denote $u_i = \partial u/\partial J_i^{\bar{\epsilon}}$ and $u_{ij} = \partial^2 u/\partial J_i^{\bar{\epsilon}} \partial J_j^{\bar{\epsilon}}$ respectively, and not first-order and second-order tensors. The operator $\mathcal{L}$ is given in indicial form by

$$\mathcal{L}(\Gamma_{ijkl}) = \frac{1}{4}\left(\Gamma_{ikjl} + \Gamma_{kijl} + \Gamma_{iklj} + \Gamma_{kilj}\right) \tag{9}$$

and the orthonormal eigenprojectors $\mathbb{E}^{\mathrm{iso}}$ and $\sqrt{5}\mathbb{E}^{\mathrm{sd}}$, are given in indicial form by

$$\begin{aligned} \mathbb{E}^{\mathrm{iso}} &= \frac{1}{3}\delta_{ij}\delta_{kl}, \\ \sqrt{5}\mathbb{E}^{\mathrm{sd}} &= \frac{1}{2}(\delta_{ik}\delta_{jl} + \delta_{il}\delta_{jk}) - \frac{1}{3}\delta_{ij}\delta_{kl}. \end{aligned} \tag{10}$$

When acting on a second-order tensor $\boldsymbol{A}$, $\mathbb{E}^{\mathrm{iso}}$ and $\sqrt{5}\mathbb{E}^{\mathrm{sd}}$ return the isotropic part of $\boldsymbol{A}$ and the symmetric deviatoric part of $\boldsymbol{A}$, respectively. The factor of $\sqrt{5}$ is introduced so that both $\mathbb{E}^{\mathrm{iso}}$ and $\mathbb{E}^{\mathrm{sd}}$ are unit tensors, thus making them an orthonormal basis for the linear manifold of all minor-symmetric fourth-order tensors. This fact is later exploited to quantify the degree of anisotropy. Using the right Cauchy–Green stretch tensor as a deformation measure, Marsden and Hughes (1994) gives a similar representation of the elastic stiffness to that of (8)

2.1. Elastic stiffness isotropy

If the elastic stiffness is presumed isotropic, by the representation theorem (Smith, 1971) of fourth-order isotropic tensors, it is expressible as

$$\mathbb{C}^{\mathrm{iso}} = 3k\mathbb{E}^{\mathrm{iso}} + 2\mu\sqrt{5}\mathbb{E}^{\mathrm{sd}}, \tag{11}$$

where k and μ are the tangent bulk and shear moduli, respectively, modulo a factor of $J = \det \boldsymbol{F}$ (where $\boldsymbol{F}$ is the deformation gradient) depending on the definition of $\bar{\boldsymbol{\epsilon}}$.

2.2. Necessary conditions for elastic stiffness isotropy

It is natural to consider the conditions under which the elastic stiffness of an isotropic material is itself isotropic. Comparing tensor coefficients of (8) and (11), and since $\bar{\boldsymbol{\gamma}}\boldsymbol{\delta}$, $\boldsymbol{\delta}\bar{\boldsymbol{\gamma}}$, $\bar{\boldsymbol{\gamma}}\bar{\boldsymbol{\gamma}}$, $\bar{\boldsymbol{h}}\boldsymbol{\delta}$, $\boldsymbol{\delta}\bar{\boldsymbol{h}}$, $\bar{\boldsymbol{h}}\bar{\boldsymbol{\gamma}}$, $\bar{\boldsymbol{\gamma}}\bar{\boldsymbol{h}}$, and $\bar{\boldsymbol{h}}\bar{\boldsymbol{h}}$ are not expressible as linear combinations of the basis tensors $\mathbb{E}^{\mathrm{iso}}$ and $\mathbb{E}^{\mathrm{sd}}$, the following conditions must be satisfied for elastic stiffness isotropy

$$u_{11} = k, \tag{12a}$$

$$u_2 = 2\mu, \tag{12b}$$

$$u_{12} = u_{22} = u_{13} = u_{23} = u_{33} = u_3 = 0. \tag{12c}$$

Substituting (12b) into (12c) implies that

$$\frac{\partial \mu}{\partial J_1^{\bar{\epsilon}}} = \frac{\partial \mu}{\partial J_2^{\bar{\epsilon}}} = \frac{\partial \mu}{\partial J_3^{\bar{\epsilon}}} = 0. \tag{13}$$

A necessary and sufficient condition for (13) to be satisfied is that μ be independent of the deformation measure. (12a) and (12c) also imply that $k = k(J_1^{\bar{\epsilon}})$. Thus, an isotropic elastic material in a distorted state will have an isotropic elastic stiffness if and only if its shear modulus is constant and bulk modulus varies at most with $J_1\bar{\boldsymbol{\epsilon}}$. Hueckel arrived at a similar conclusion with respect to the secant bulk and shear moduli (Hueckel et al., 1992).

For elastic–plastic materials, similar analysis implies that μ is independent of the deformation measure but can still depend on η and q_k. This may be a means of accounting for apparent dependence of μ on pressure through elastic–plastic coupling, though this is not considered further in this paper.

2.3. First order approximation of $\mathbb{C}$

In this and subsequent sections, the first-order approximation of $\mathbb{C}$ in (8)

$$\mathbb{C} = 3u_{11}\mathbb{E}^{\text{iso}} + u_2\sqrt{5}\mathbb{E}^{\text{sd}} + u_{12}(\bar{\boldsymbol{\gamma}}\boldsymbol{\delta} + \boldsymbol{\delta}\bar{\boldsymbol{\gamma}}) \tag{14}$$

is adopted. Comparing tensor coefficients of (14) to (8), the derivatives of the strain energy can be given in terms of the familiar bulk and shear modulus

$$u_{11} = k(J_1^{\bar{\epsilon}}) \tag{15a}$$

$$u_2 = 2\mu(J_1^{\bar{\epsilon}}) \tag{15b}$$

$$u_{12} = 2\frac{d\mu(J_1^{\bar{\epsilon}})}{dJ_1^{\bar{\epsilon}}} = 2\mu'. \tag{15c}$$

where the μ' indicates differentiation with respect to $J_1^{\bar{\epsilon}}$.

2.3.1. Elastic compliance

In numerical constitutive models, the fourth-order elastic compliance tensor $\mathbb{S} = \mathbb{C}^{-1}$ is needed to evaluate the elastic strain increment when the stress increment is known. Successive application of the Sherman–Morrison formula (Golub

Input Unrotated Cauchy stress $\boldsymbol{\sigma}_{\text{old}}$, unrotated (approximate) strain increment $d\boldsymbol{\varepsilon} = \boldsymbol{d}\Delta t$, timestep Δt, Jacobian J_{old}, elastic strain $\boldsymbol{\varepsilon}^{\text{e}}{}_{\text{old}}$.

Output Cauchy stress $\boldsymbol{\sigma}_{\text{new}}$

Step 1 Compute trial Kirchhoff stress

$$\boldsymbol{\tau}^{\text{trial}} = J_{\text{old}}\boldsymbol{\sigma}_{\text{old}} + \kappa(\varepsilon_{\text{v}})d\varepsilon_{\text{v}}\boldsymbol{\delta} + 2\mu(\varepsilon_{\text{v}})d\boldsymbol{\gamma} + \langle\langle 2\mu'\,(d\varepsilon_{\text{v}}\boldsymbol{\gamma}^{\text{e}}{}_{\text{old}} + \boldsymbol{\gamma}^{\text{e}}{}_{\text{old}}{:}d\boldsymbol{\varepsilon}\boldsymbol{\delta})\rangle\rangle$$

Step 2 Check yield condition

if $f\left(\boldsymbol{\tau}^{\text{trial}}\right) \le 0$ **then**

$$\boldsymbol{\tau} = \boldsymbol{\tau}^{\text{trial}}, \quad d\boldsymbol{\varepsilon}^{\text{e}} = d\boldsymbol{\varepsilon}, \quad d\boldsymbol{\varepsilon}^{\text{p}} = \boldsymbol{0}$$

go to Step 6

endif

Step 3 Compute yield normal, flow direction, and return direction

$$\boldsymbol{n} = \frac{\partial f/\partial\boldsymbol{\tau}}{\|\partial f/\partial\boldsymbol{\tau}\|}, \qquad \boldsymbol{m} = \frac{\partial\varphi/\partial\boldsymbol{\tau}}{\|\partial\varphi/\partial\boldsymbol{\tau}\|},$$

$$\boldsymbol{p} = \kappa(\varepsilon_{\text{v}})\,\text{tr}\,\boldsymbol{m}\boldsymbol{\delta} + 2\mu(\varepsilon_{\text{v}})\,\text{dev}\,\boldsymbol{m} - J_{\text{old}}\boldsymbol{\sigma}_{\text{old}}{:}\boldsymbol{m}\boldsymbol{\Gamma} + \langle\langle 2\mu'\,(\text{tr}\,\boldsymbol{m}\boldsymbol{\gamma}^{\text{e}}{}_{\text{old}} + \boldsymbol{\gamma}^{\text{e}}{}_{\text{old}}{:}\boldsymbol{m}\boldsymbol{\delta})\rangle\rangle$$

Step 4 Improve estimates for stress and check convergence

$$\boldsymbol{\tau} = \boldsymbol{\tau}^{\text{trial}} - \frac{f\left(\boldsymbol{\tau}^{\text{trial}}\right)}{(\partial f/\partial\boldsymbol{\tau}){:}\boldsymbol{p}}\boldsymbol{p}$$

if $\left\|\boldsymbol{\tau} - \boldsymbol{\tau}^{\text{trial}}\right\| >$ `TOL` **then**

$$\boldsymbol{\tau}^{\text{trial}} = \boldsymbol{\tau}$$

go to Step 3

endif

Step 5 Update elastic and plastic strain

$$\left\langle\left\langle \varkappa = 4\frac{J_2^{\varepsilon}\mu'}{\kappa\mu}\right\rangle\right\rangle, \quad \left\langle\left\langle \zeta = \frac{3}{2}\frac{\kappa\mu(1-\varkappa)}{\mu'}\right\rangle\right\rangle$$

$$\left\langle\left\langle \alpha_1 = \frac{1}{\zeta}\left(\frac{2}{3}J_2^{\varepsilon}\frac{\text{tr}\,d\boldsymbol{\tau}}{\kappa} - \frac{\boldsymbol{\gamma}^{\text{e}}{}_{\text{old}}{:}d\boldsymbol{\tau}}{2\mu'}\right)\right\rangle\right\rangle, \quad \left\langle\left\langle \alpha_2 = \frac{1}{\zeta}\left(\frac{3}{2}J_2^{\varepsilon}\frac{\boldsymbol{\gamma}^{\text{e}}{}_{\text{old}}{:}d\boldsymbol{\tau}}{\mu} - \frac{\text{tr}\,d\boldsymbol{\tau}}{2\mu'}\right)\right\rangle\right\rangle$$

$$d\boldsymbol{\varepsilon}^{\text{e}} = \frac{1}{3\kappa}\,\text{tr}\,d\boldsymbol{\tau}\boldsymbol{\delta} + \frac{1}{2\mu}\,\text{dev}\,d\boldsymbol{\tau} + \langle\langle\alpha_1\boldsymbol{\delta} + \alpha_2\boldsymbol{\gamma}^{\text{e}}{}_{\text{old}}\rangle\rangle$$

$$d\boldsymbol{\varepsilon}^{\text{p}} = d\boldsymbol{\varepsilon} - d\boldsymbol{\varepsilon}^{\text{e}}$$

Step 6 Update energy, temperature, Jacobian, and all other state variables to end of step

Step 7 Convert updated Kirchhoff stress to Cauchy stress

$$\boldsymbol{\sigma} = \frac{1}{J}\boldsymbol{\tau}$$

Fig. 1. Elastic–plastic Kirchhoff stress-update algorithm. New terms involving recoverable deformation induced anistropy, not expected to be included in an existing stress-update algorithm, are set apart explicitly by $\langle\langle\bullet\rangle\rangle$ in Steps 1, 3, and 5.

et al., 1996) for the inversion of a rank-one modification of a tensor allows the rank-two modification in (14) to be inverted to give

$$\mathbb{S} = \frac{1}{3k}\mathbb{E}^{\text{iso}} + \frac{\sqrt{5}}{2\mu}\mathbb{E}^{\text{sd}} - \frac{1}{\phi}\left[3k\mu\mu'(\bar{\boldsymbol{\gamma}}\boldsymbol{\delta} + \boldsymbol{\delta}\bar{\boldsymbol{\gamma}}) - (\mu')^2\left(9k\bar{\boldsymbol{\gamma}}\bar{\boldsymbol{\gamma}} + 4\mu J_2^{\bar{\epsilon}}\boldsymbol{\delta}\boldsymbol{\delta}\right)\right], \tag{16}$$

where

$$\phi = 9k\mu\left(k\mu - 4J_2^{\bar{\epsilon}}(\mu')^2\right). \tag{17}$$

3. Incorporation of recoverable deformation induced anisotropy in a classical elastic–plastic framework

For strain increment driven models, Fig. 1 implements RDIA in the elastic stiffness and compliance for isotropic elastic–plastic materials in a classical elastic–plastic framwork as described by Brannon (2007).

As can be seen in Steps 1, 3, and 5 of Fig. 1, endowing the effects of RDIA on an existing elastic–plastic model is a matter of adding very few easily evaluated terms. The only terms which are not readily available in most finite element host codes are the elastic strains, which can be easily carried as internal state variables to the model for a moderate additional computational cost.

4. Quantification of anisotropy

As proved in the previous section, the elastic stiffness of isotropic elastic and elastic–plastic materials must develop RDIA in its integrity basis in response to distortion. The degree of the resultant anisotropy is now quantified by a single scalar ψ for several classes of engineering materials.

The notion of quantifying the degree of anisotropy of a tensor by a single scalar measure has previously been considered in a number of contexts and disciplines (Backus, 1970; Nye, 1957; Pierpaoli & Basser, 1996; Rychlewski, 1984). Though the formulations differ in their details, they share the common objective of attempting to quantify, in a meaningful way, the degree to which the tensor *is not* isotropic. Commonly, ψ is defined by the ratio of the norm of the difference between a tensor $\boldsymbol{\mathcal{A}}$ and its isotropic part and the norm of $\boldsymbol{\mathcal{A}}$ (Fedorov, 1968)

$$\psi(\boldsymbol{\mathcal{A}}) = \frac{\|\boldsymbol{\mathcal{A}} - \boldsymbol{\mathcal{A}}^{\text{iso}}\|}{\|\boldsymbol{\mathcal{A}}\|}, \tag{18}$$

where $\boldsymbol{\mathcal{A}}^{\text{iso}}$, the isotropic part of $\boldsymbol{\mathcal{A}}$, is given by

$$\boldsymbol{\mathcal{A}}^{\text{iso}} = \mathcal{P}\cdot\boldsymbol{\mathcal{A}} \tag{19}$$

and $\mathcal{P}$ is the tensor projector which projects $\boldsymbol{\mathcal{A}}$ on to the hyper-surface spanned by the isotropic basis for nth-order tensors and $\cdot$ represents the appropriate order tensor contraction.

In this form, ψ has previously been used in a variety of applications, for example, in the investigation of crystal optics where the degree of anisotropy has important implications on the behavior of light in anisotropic crystals (Fedorov, 1968), second-order tensors in mechanics (Rychlewski, 1984; Zhang, 1990), and finding the isotropic tensor closest to an anisotropic symmetry (Moakher & Norris, 2006; Norris, 2006b).

Rather than adopt (18), (Brannon, 2009) makes the following observation: given a tensor $\boldsymbol{\mathcal{A}}$, $\boldsymbol{\mathcal{A}}^{\text{iso}}$ is the projection of $\boldsymbol{\mathcal{A}}$ onto the hyper-surface spanned by the unit basis tensors of the isotropic part of $\boldsymbol{\mathcal{A}}$. For fourth-order tensors, the basis tensors are given by $\mathbb{E}^{\text{iso}}$ and $\sqrt{5}\mathbb{E}^{\text{sd}}$, and a geometric description of the projection is shown in Fig. 2.

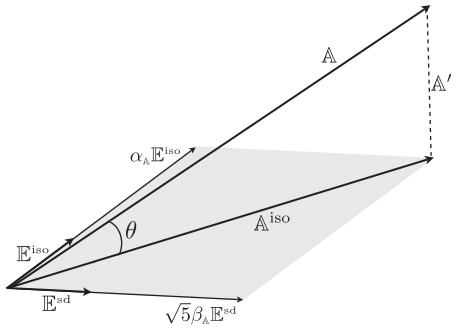

Fig. 2. Geometric interpretation of decomposition of fourth-order tensor into isotropic and non-isotropic parts, showing the angle θ between the tensor $\mathbb{A}$ and the isotropic hyper-plane.

The angle θ between $\boldsymbol{\mathcal{A}}$ and $\boldsymbol{\mathcal{A}}^{\text{iso}}$, defined analogously to the angle between two vectors, is given by

$$\cos\theta = \frac{\boldsymbol{\mathcal{A}} :: \boldsymbol{\mathcal{A}}^{\text{iso}}}{\|\boldsymbol{\mathcal{A}}\|\|\boldsymbol{\mathcal{A}}\|} = \frac{\|\boldsymbol{\mathcal{A}}^{\text{iso}}\|}{\|\mathcal{A}\|}. \tag{20}$$

Rearranging and normalizing, the scalar measure of anisotropy is defined as

$$\psi\boldsymbol{\mathcal{A}} = \frac{2}{\pi}\cos^{-1}\left(\frac{\|\boldsymbol{\mathcal{A}}^{\text{iso}}\|}{\|\mathcal{A}\|}\right), \tag{21}$$

4.0.2. Properties of ψ

As given in (21), ψ has the following properties:

$$\psi(\boldsymbol{\mathcal{A}}^{\text{iso}}) = 0, \quad \psi(\boldsymbol{\mathcal{A}}') = 1,$$

$$\psi(\boldsymbol{\mathcal{A}}) \geqslant 0,$$

$$\psi(\alpha\boldsymbol{\mathcal{A}}) = \alpha\psi(\boldsymbol{\mathcal{A}}), \quad \alpha \in \mathbb{R},$$

$$\psi(\mathbf{Q} * \boldsymbol{\mathcal{A}}) = \psi(\mathcal{A}).$$

Because ψ is based on the Euclidean norm, ψ is not invariant under inversion (Norris, 2006a), i.e.,

$$\psi(\boldsymbol{\mathcal{A}}^{-1}) \neq \psi(\boldsymbol{\mathcal{A}}). \tag{22}$$

However, several of the previous alternative measures suffer from the same problem. If invariance under inversion is required, ψ may be replaced with

$$\psi^{\dagger}(\boldsymbol{\mathcal{A}}) = \frac{1}{2}(\psi(\boldsymbol{\mathcal{A}}) + \psi(\boldsymbol{\mathcal{A}}^{-1})) \tag{23}$$

which is invariant under inversion. Despite this drawback, (21) is adopted due to its intuitive geometric interpretation and computational ease.

4.1. Degree of anisotropy in several inherently anisotropic materials

For perspective in the subsequent sections in which the degree of RDIA in isotropic elastic–plastic materials is quantified, the degree of anisotropy ψ of the elastic stiffness of several inherently anisotropic materials is shown plotted against $\|\mathbb{C}^{\text{iso}}\|/\|\mathbb{C}\|$ in Fig. 3 for uniaxial strain compression. The coefficients for the elastic stiffnesses of each material shown in Fig. 3 are taken from Böhlke and Brüggemann (2001) and the references therein.

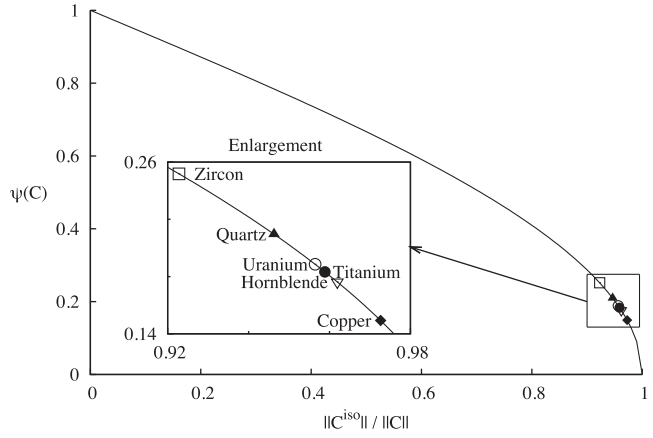

Fig. 3. Measure of anisotropy $\psi(\mathbb{C})$ for Zircon 22,251 □ (tetragonal symmetry), Quartz 62,894 ▲ (trigonal symmetry), Uranium ○ (orthorhombic symmetry), Titanium 52,743 • (hexagonal symmetry), Hornblende 42,420 ▽ (monoclinic symmetry), and Copper ♦ (cubic symmetry). Material data from Böhlke and Brüggemann (2001).

4.2. Degree of recoverable deformation induced anisotropy in isotropic media

In contrast to the materials in Fig. 3, whose degree of anisotropy is inherent and constant, the degree of anisotropy in isotropic elastic materials varies with deformation. As will be shown, the degree of RDIA in classical elastic–plastic materials generally depends on two competing constitutive factors: pressure dependence of the shear modulus and pressure-dependence of the yield function. These two features will be explored in this section.

4.2.1. Constitutive model

The yield function in Fig. 1 is given by the pressure-dependent form

$$f(\bar{\boldsymbol{\sigma}}) = \sqrt{J_2^{\bar{\sigma}}} - a_1 + a_3 e^{a_2 J_1^{\bar{\sigma}}} + a_4 J_1^{\bar{\sigma}} + a_5 \left(\gamma_{\text{eq}}^{\text{p}}\right)^m, \tag{24}$$

where a_1–a_5 and m are material parameters, and $\gamma_{\text{eq}}^{\text{p}}$ is the equivalent plastic strain. As defined, f is capable of reducing to several common plasticity models, e.g., choosing a_2–a_4 equal to zero, J_2 plasticity with isotropic strain hardening is recovered, choosing a_2, a_3, and a_5 equal to zero, linear Drucker–Prager plasticity is recovered. or, if a_5 is set equal to zero, the yield function employed by the Sandia Geomodel (Brannon, Fossum, & Strack, 2009; Fossum & Brannon, 2004, 2006) is recovered.

The bulk modulus and shear modulus are taken as

$$k = k_0 - k_0 \left.\frac{dk}{dp}\right|_0 J_1^{\bar{\epsilon}}. \tag{25}$$

$$\mu = \mu_0 - k_0 \left.\frac{d\mu}{dp}\right|_0 J_1^{\bar{\epsilon}}. \tag{26}$$

In Eqs. (25) and (26), since elastic moduli are typically measured as functions of pressure, use has been made of the chain rule to cast first order bulk and shear moduli coefficients in terms of pressure derivatives.

Applying (19) to the reduced elastic stiffness of (14), the isotropic part of $\mathbb{C}$ is given by $\mathbb{C}^{\text{iso}}$ in (11), and $\psi\mathbb{C}$ is reducible to

$$\psi(\mathbb{C}) = \frac{2}{\pi} \cos^{-1}\left(\frac{9k^2 + 5(2\mu)^2}{9k^2 + 5(2\mu)^2 + 12(2\mu')^2 J_2^{\epsilon}}\right) \tag{27}$$

4.2.2. Degree of recoverable deformation induced anisotropy in elastic materials

The degree of anisotropy for an elastic material subjected to uniaxial strain compression is shown in Fig. 4. Parameters for the constitutive model are $k_0 = 237$ GPa, $\mu_0 = 246$ GPa, $d\mu/dp|_0 = 9$, $dk/dp|_0 = 2$. Yield was suppressed by taking a_4 to be an arbitrarily large number.

The data in Fig. 4 demonstrate that, for elastic loading, the magnitude of anisotropy induced by deformation in isotropic materials is capable of attaining and even exceeding the magnitude of anisotropy in intrinsically anisotropic materials at finite strains.

4.2.3. Degree of recoverable deformation induced anisotropy in elastic–plastic materials

Of course, in elastic–plastic materials, due to the limit on the magnitude of realizable elastic deviatoric strain imposed by the yield criterion, the magnitude of RDIA will also be limited. As an illustration, the degree of RDIA for the same material as

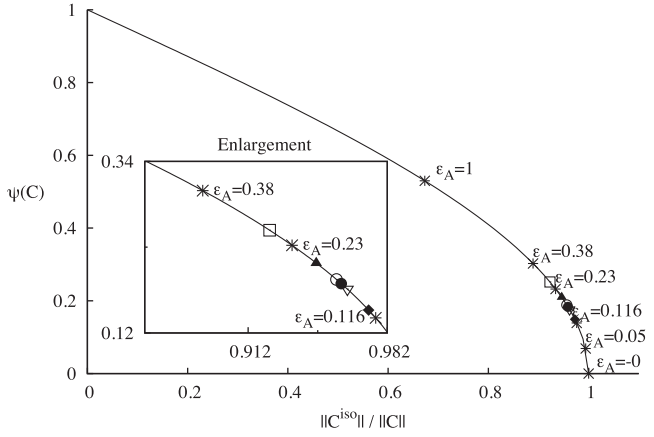

Fig. 4. Variation of the measure of anisotropy $\psi(\mathbb{C})$ for elastic uniaxial strain deformation $*$. Also shown are $\psi(\mathbb{C})$ for Zircon 22,251 □ (tetragonal symmetry), Quartz 62,894 ▲ (trigonal symmetry), Uranium ○ (orthorhombic symmetry), Titanium 52,743 • (hexagonal symmetry), Hornblende 42,420 ▽ (monoclinic symmetry), and Copper ♦ (cubic symmetry).

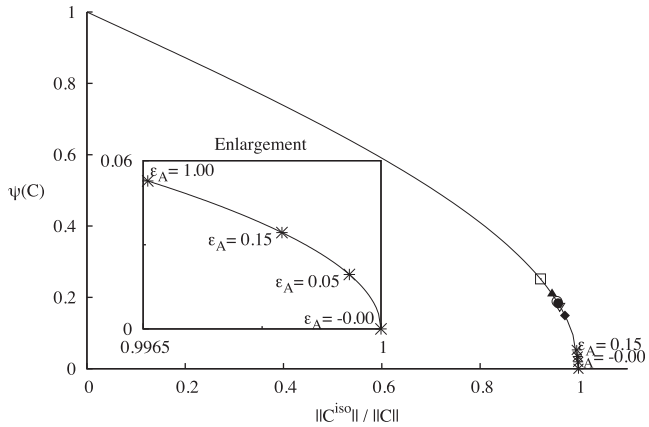

Fig. 5. Variation of the measure of anisotropy for uniaxial strain deformation for the same material as in Fig. 4 but allowing for plastic yielding ∗. Also shown are $\psi(\mathbb{C})$ for Zircon 22,251 □ (tetragonal symmetry), Quartz 62,894 ▲ (trigonal symmetry), Uranium ○ (orthorhombic symmetry), Titanium 52,743 • (hexagonal symmetry), Hornblende 42,420 ▽ (monoclinic symmetry), and Copper ♦ (cubic symmetry).

Section 4.2.2 and subjected to the same uniaxial strain compression, is shown in Fig. 5 allowing for yield by taking a_1 = 1800 MPa and a_4 = 0.095.

As illustrated in Fig. 5, allowing for yield limits the degree of RDIA in this material quite severely. Only at very large strains does the degree of anisotropy even exceed 5%.

4.2.4. Factors affecting the degree of recoverable deformation induced anisotropy in isotropic materials

Considering the term involving RDIA in the elastic stiffness in (14),

$$\mathbb{C}^{\mathrm{RDIA}} = 2\mu'(\bar{\gamma}^{\mathrm{e}}\boldsymbol{\delta} + \boldsymbol{\delta}\bar{\gamma}^{\mathrm{e}}), \tag{28}$$

two key factors in how large the magnitude of RDIA becomes during loading are: pressure-dependence of the shear modulus, and, implicitly, the pressure dependence of yield which allows the realizable elastic deviatoric strain to increase with pressure. It turns out that under some circumstances these two are competing factors. In the following paragraphs, each factor will be considered separately using the same model parameters as used in Fig. 5.

Pressure-dependence of the shear modulus. In Fig. 6, the magnitude of RDIA is shown plotted versus axial strain for uniaxial strain deformation for varying $d\mu/dp$. All other model parameters are the same as for the material in Fig. 5.

Referring to Fig. 6, increasing dependence of the shear modulus on pressure through increasing values of $d\mu/dp$ does not necessarily lead to an increase in the magnitude of RDIA at all strains. This behavior is explained by observing that stronger dependence of the shear modulus on pressure results in an increase in deviatoric strain at a given pressure. Thus, unless the pressure-dependence of strength is also large, the elastic-deviatoric strain will decrease with increasing pressure due to the yield criterion, causing a decrease in the magnitude of $\mathbb{C}^{\mathrm{RDIA}}$. Depending relative competing effects of pressure-dependence of

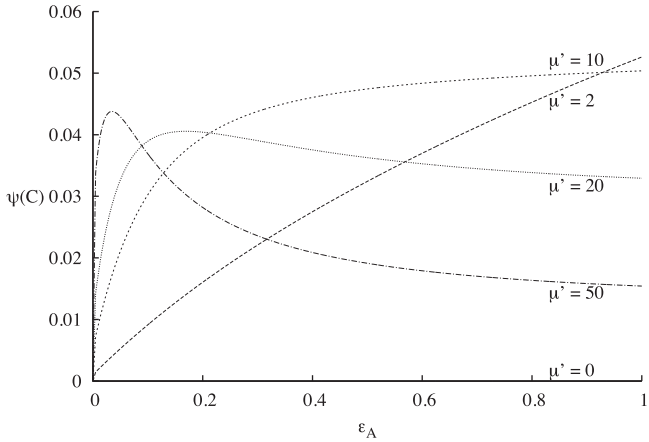

Fig. 6. Variation of the measure of anisotropy $\psi(\mathbb{C})$ with μ' for uniaxial strain deformation plotted against axial strain for $d\mu/dp$ = 50-·-·-·-·-, $d\mu/dp$ = 20. . . . . , $d\mu/dp$ = 10------, $d\mu/dp$ = 2—–—–—, and $d\mu/dp$ = 0.0—. For large values of $\mu', \psi(\mathbb{C})$ decreases due to the limiting value of shear strain.

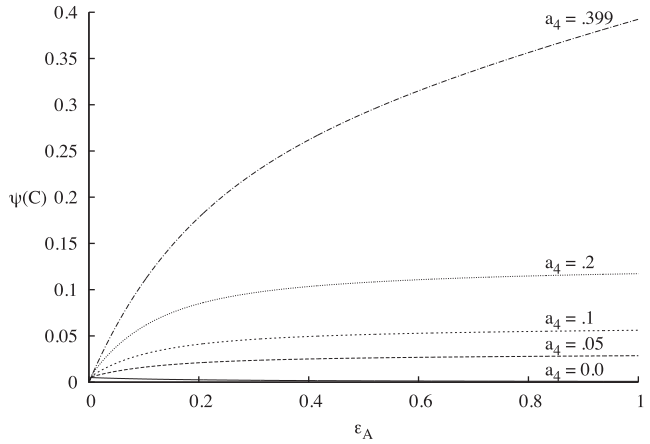

Fig. 7. Variation of the measure of anisotropy $\psi(\mathbb{C})$ with a_4 for uniaxial strain deformation plotted against axial strain for $a_4 = 0.399$-·-·-·-·-, $a_4 = 0.2$. . . . . , $a_4 = 0.1$- - - - - - -, $a_4 = 0.05$— - - - —, and $a_4 = 0.0$—. Except for the largest values of a_4, $\psi(\mathbb{C})$ never exceeds 5%.

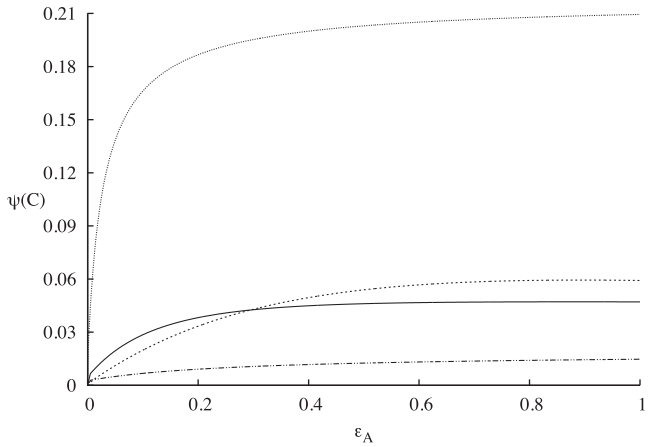

Fig. 8. Degree of recoverable anisotropy in elastic–plastic materials in triaxial strain compression for linearly pressure-dependent elastic moduli for TiB_2—, limestone- - - - - -, and 2024 aluminum-·-·-·-·-. With the exception of alumina, the degree of recoverable anisotropy never exceeds 5% even in the finite strain regime.

strength and shear modulus, even materials with moderate pressure-dependence of shear modulus can exhibit large degrees of RDIA at large strains.

Pressure-dependence of the yield. In Fig. 7, the magnitude of RDIA is shown plotted versus axial strain for uniaxial strain deformation for increasing levels of pressure dependence of strength achieved by varying a_4. All other model parameters are the same as for the material in Fig. 5. Based on the observation of Lee, Brannon, and Bronowski (2004) that the slope of the yield function in stress space never exceeded the slope of the stress trajectory for uniaxial strain loading, the upper limit of $a_4 = 0.399$ was chosen as this limiting value.

Not surprisingly, since the size of the elastic domain increases monotonically with a_4, the degree of RDIA also increases at all strains monotonically with a_4.

4.3. Magnitude of recoverable deformation induced anisotropy in a selection of engineering materials

It has been shown that, for pressure-sensitive materials, the RDIA of the elastic stiffness can be comparable in magnitude to the degree of anisotropy in inherently anisotropic materials in the finite strain regime for elastic loading, though its magnitude was severely restricted when allowing for yield. The degree of RDIA is shown in Fig. 8 for limestone, 2024 aluminum, TiB_2, and 99.5% alumina whose properties are outlined in Table 1 for uniaxial and triaxial $\bar{\boldsymbol{\epsilon}} = (\bar{\epsilon}, \bar{\epsilon}/10, \bar{\epsilon}/10, 0, 0, 0)^{\mathrm{T}}$ strain compression.

Though the magnitude of RDIA is characterized for the specific materials outlined, they were chosen to be representative of the larger classes of geologic, ceramic, metallic, and powdered metal materials, respectively.

Table 1
Material properties representative of ceramic, geologic, and metallic materials used in simulations shown in Fig. 8.

Property	Material			
	TiB_2[a]	Limestone[b]	2024 Al[c]	99.5% alumina[d]
k_0 (GPa)	237.0	24.0	76.0	1.549
μ_0 (GPa)	246.0	15.1	28.6	2.722
$\partial\mu/\partial p\|_0$	9.0	2	1.8	208.5
$\partial k/\partial p\|_0$	2.0	0	4.75	171.6
a_1 (MPa)	1800	71.9	256.0	4.2
a_2 (1/MPa)	0.0	3180.0	0.0	0.0
a_3 (MPa)	0.0	70.1	0.0	0.0
a_4	0.095	0.171	0.0017	0.1813
a_5 (MPa)	0.0	0.0	426	0.0
m	NA	NA	0.34	NA

[a] Data from Grady (1991).
[b] Data from Brannon et al. (2009).
[c] Data from Johnson and Cook (1985), Steinberg (1996).
[d] Data from Zeuch et al. (2001).

5. Discussion and summary

In initially isotropic materials whose shear modulus and strength vary with pressure, the degree of RDIA increases with axial strain in uniaxial and triaxial strain deformation. The degree of RDIA is not sensitive to the loading paths investigated, being nearly the same in uniaxial and triaxial compression. For the metallic, geologic, ceramic, and powdered metal materials investigated, the following general observations can be made:

- For metallic materials, even with the inclusion of slight pressure-dependence of yield as reported by Richmond and Spitzig (1980), the degree of RDIA is, even at finite strains, negligible. This observation makes sense in light of the observation that the ratio of strength and shear modulus is constant (Hua et al., 2002) in metals, which limits the elastic-deviatoric strain from achieving magnitudes which allow for the development of RDIA in the material.
- For geologic materials, in which the strength and shear modulus are both moderately dependent on pressure, the magnitude of RDIA is significant only in large deformation, finite strain, regimes. If a geologic material is incapable of withstanding such large deformations without catastrophic failure, or is only exercised in small strain regimes, the effects of RDIA are negligible.
- For ceramic materials, in which the strength and shear modulus can both be strongly dependent on pressure, the magnitude of RDIA can potentially become significant at moderate strains. However, like the geologic materials, the ceramic material would have to be capable of withstanding even these moderate levels of strain for RDIA to be significant without failing.
- For the powdered metals in which the strength and shear modulus are extremely pressure-dependent, the degree of RDIA is significant even at small strains.

5.1. Summary

The distinction between isotropic functions and isotropic tensors was emphasized. An isotropic material is one in which its internal energy is an isotropic function of the invariants of the strain tensor. Twice differentiating this isotropic energy function results in thermodynamically required deformation-induced anisotropy in the fourth-order elastic stiffness. The stiffness will be anisotropic except in the case that the bulk modulus varies at most with J_1^e and the shear modulus is constant. Considering laboratory evidence that μ is not constant, even in common engineering materials (Duffy, Shen, Shu, Hemley, & Singh, 1999; Guinan & Steinberg, 1975; Hayes et al., 1999), the assumption of isotropy of the elastic stiffness should be abandoned to allow revised analysis of material characterization data in a thermodynamically consistent manner. In other words, if using an isotropic stiffness leads to a pressure-dependent shear modulus, then the data must be re-analyzed allowing for RDIA, or irreversible changes in pressure in pressure associated with dissipation rather than elastic volume change.

RDIA is only one source of deformation induced anisotropy. For ceramics and rocks, which fail through growth of oriented cracks, inelastic deformation-induced anisotropy is expected to be severe. Nevertheless, the inclusion of RDIA in a computational framework is only a matter of adding a few extra lines of easily evaluated code to existing models, as shown in Fig. 1, and should, therefore, be included if thermodynamic admissibility is a desired attribute of the computational model.

References

Backus, G. (1970). A geometrical picture of anisotropic elastic tensors. *Reviews of Geophysics and Space Physics, 8*(3), 633–671.
Böhlke, T., & Brüggemann, C. (2001). Graphical representation of the generalized Hooke's law. *Technishe Mechanik, 21*(2), 145–158.

Borja, R. I., Tamagnini, C., & Amorosi, A. (1997). Coupling plasticity and energy conserving elasticity models for clays. *Journal of Geotechnical Geoenvironmental Engineering, 123*(10), 948–957.
Brannon, R. M. (2007). Elements of phenomenological plasticity: Geometrical insight, computational algorithms, and topics in shock physics. In Y. Horie (Ed.). *Shock Wave Science and Technology Reference Library* (Vol. 2, pp. 225–274). Berlin: Springer.
Brannon, R. M. (2009). Functional and structured tensor analysis for engineers. Available from: <http://mech.utah.edu/brannon/public/Tensors.pdf>.
Brannon, R., Fossum, A., & Strack, O. (2009). Kayenta: Theory and User's Guide. Tech. Rep. SAND2009-2282, Sandia National Laboratory.
Burakovsky, L., Greeff, C. W., & Preston, D. L. (2003). Analytic model of the shear modulus at all temperatures and densities. *Physical Review B, 67*(094107), 1–9.
Collins, I., & Houlsby, G. (1997). Application of thermomechanical principles to the modeling of geotechnical materials. *Proceedings of the Royal Society of London, 453*, 1975–2001.
Duffy, T. S., Shen, G., Shu, J., Hemley, R. J., & Singh, A. K. (1999). Elasticity, shear strength, and equation of state of molybdenum and gold from x-ray diffraction under nonhydrostatic compression to 24 gpa. *Journal of Applied Physics, 86*(12), 6729–6736.
Einav, I., & Puzrin, A. M. (2004). Pressure-dependent elasticity and energy conservation in elastoplastic models for soils. *Journal of Geotechnical Geoenvironmental Engineering, 130*(1), 81–92.
Fedorov, F. J. (1968). *Theory of elastic waves in crystals*. Plenum Press.
Fossum, A., & Brannon, R. (2004). *Unified compaction/dilation, strain-rate sensitive, constitutive model for rock mechanics structural analysis applications*. *Rock Mechanics Across Borders and Disciplines. No. ARMA/NARMS 04-546*. American Rock Mechanics Association.
Fossum, A., & Brannon, R. (2006). On a viscoplastic model for rocks with mechanism-dependent characteristic times. *Acta Geotechnica, 1*(2), 89–106.
Golub, G. H., & Van Loan, C. F. (1996). *Matrix computations (Johns Hopkins studies in mathematical sciences)* (3rd ed.). The Johns Hopkins University Press<http://www.worldcat.org/isbn/0801854148> .
Grady, D. (1991). Shock compression properties of ceramics. SAND Report SAND-91-1474C, Sandia National Laboratory.
Guinan, M., & Steinberg, D. (1975). A simple approach to extrapolating measured polycrystalline shear moduli to very high pressure. *Journal of Physics and Chemistry of Solids, 36*(7–8), 829.
Hayes, D., Hixson, R., & McQueen, R. (1999). *High pressure elastic properties, solid–liquid phase boundary and liquid equation of state from release wave measurements in shock-loaded copper*. *Shock Compression of Condensed Matter* (Vol. 505). AIP.
Hill, R. (1948). A theory of the yielding and plastic flow of anisotropic metals. *Proceedings of the Royal Society of London, 193*(1033), 281–297.
Horii, H., & Nemat-Nasser, S. (1983). Overall moduli of solids with microcracks: Load-induced anisotropy. *Journal of Mechanics and Physics of Solids, 31*(2), 155–171.
Houlsby, G. T. (1985). The use of a variable shear modulus in elastic–plastic models for clays. *Computer Geotechnics, 1*(1), 3–13.
Houlsby, G. T., Amorosi, A., & Rojas, E. (2005). Elastic moduli of soils dependent on pressure: A hyperelastic formulation. *Geotechnique, 55*, 383–392.
Hua, J., Jing, F., Hua, T., & Hu, S. (2002). Is the empirical approximation y/g = constant applicable to high-pressure and high-temperature environments for metals? *Journal of Physics: Condensed Matter, 14*, 10843–10848.
Hueckel, T., Tutumluer, E., & Pellegrini, R. (1992). A note on non-linear elasticity of isotropic overconsolidated clays. *International Journal for Numerical and Analytical Methods in Geomechanics, 16*, 603–618.
Johnson, G., Cook, W. (1985). A constitutive model and data for metal subjected to large strains, high strain rates, and high temperatures. In *7th international symposium on ballisitics* (pp. 541–547).
Kachanov, M. (1982). A microcrack model of rock inelasticity–Part I: Frictional sliding on microcracks. *Mechanics of Materials, 1*, 19–27.
Lee, M. Y., Brannon, R. M., Bronowski, D. R. (2004). Uniaxial and triaxial compression tests of silicon carbid ceramics under quasi-static loading condition. Tech. Rep. SAND2004-6005, Sandia National Laboratory.
Malvern, L. (1969). *An introduction to the mechanics of a continuous medium*. Prentice-Hall Inc..
Marsden, J. E., & Hughes, T. J. (1994). *Mathematical foundations of elasticity*. Dover Publications.
Moakher, M., & Norris, A. N. (2006). The closest elastic tensor of arbitrary symmetry to an elasticity tensor of lower symmetry. *Journal of Elasticity, 85*(3), 215–263.
Norris, A. N. (2006a). Elastic moduli approximation of higher symmetry for the acoustical properties of an anisotropic material. *Journal of Acoustical Society of America, 119*(4), 2114–2121.
Norris, A. N. (2006b). The isotropic material closest to a given anisotropic material. *Journal of Mechanics of Materials and Structures, 1*(2), 231–246.
Nye, J. F. (1957). *Physical properties of crystals*. Oxford Clarendon Press.
Pierpaoli, C., & Basser, P. J. (1996). Toward a quantitative assessment of diffusion anisotropy. *Magnetic Resonance in Medicine, 36*, 893–906.
Richmond, O., & Spitzig, W. (1980). Pressure dependence and dilatancy of plastic flow. In F. Rimrott & B. Tabarrok (Eds.), *Theoretical and Applied Mechanics: Proceedings of the XVth International Congress of Theoretical and Applied Mechanics* (pp. 377–386). Amsterdam: North-Holland Publishing Company.
Rychlewski, J. (1984). On evaluation of anisotropy of properties described by symmetric second-order tensors. *Czechoslovak Journal of Physics, 34*, 499–506.
Scheidler, M. (1996). On the coupling of pressure and deviatoric stress in isotropic hyperelastic materials. Tech. Rep. ARL-TR-954, Army Research Laboratory.
Smith, G. (1971). On isotropic functions of symmetric tensors, skew-symmetric tensors and vectors. *International Journal of Engineering Science, 9*, 899–916.
Steinberg, D. (1996). Equation of state and strength properties of selected materials. Tech. Rep. UCRL-MA-106439, Lawerence Livermore National Laboratory.
Stouffer, D., & Bodner, S. (1979). A constitutive model for the deformation induced anisotropic plastic flow of metals. *International Journal of Engineering Science, 17*(6), 757–764.
Willam, K. J. (2002). Constitutive models for engineering materials. In *Encyclopedia of Physical Science and Technology* (3rd ed., pp. 603–633). Academic Press.
Zeuch, D., Grazier, J., Arguello, J., & Ewsuk, K. (2001). Mechanical properties and shear failure surfaces of two alumina powders in triaxial compression. *Journal of Materials Science, 36*(12), 2911–2924.
Zhang, J. (1990). Anisotropy degree in nonlinear solids. *Applied Mathematics and Mechanics, 11*(3), 239–246.
Zytynski, M., Randolph, M., Nova, R., & Wroth, C. (1978). Short communications on modeling the unloading-reloading behaviour of soils. *International Journal for Numerical and Analytical Methods in Geomechanics, 2*, 87–94.